Manganese Limitation Induces Changes in the Activity and in the Organization of Photosynthetic Complexes in the Cyanobacterium *Synechocystis* sp. Strain PCC 6803[1][C][W][OA]

Eitan Salomon and Nir Keren*

Department of Plant and Environmental Sciences, Alexander Silberman Institute of Life Sciences, Givat Ram, Hebrew University of Jerusalem, Jerusalem 91904, Israel

Manganese (Mn) ions are essential for oxygen evolution activity in photoautotrophs. In this paper, we demonstrate the dynamic response of the photosynthetic apparatus to changes in Mn bioavailability in cyanobacteria. Cultures of the cyanobacterium *Synechocystis* PCC 6803 could grow on Mn concentrations as low as 100 nM without any observable effect on their physiology. Below this threshold, a decline in the photochemical activity of photosystem II (PSII) occurred, as evident by lower oxygen evolution rates, lower maximal photosynthetic yield of PSII values, and faster Q_A reoxidation rates. In 77 K chlorophyll fluorescence spectroscopy, a peak at 682 nm was observed. After ruling out the contribution of phycobilisome and iron stress-induced IsiA proteins, this band was attributed to the accumulation of partially assembled PSII. Surprisingly, the increase in the 682-nm peak was paralleled by a decrease in the 720-nm peak, dominated by PSI fluorescence. The effect on PSI was confirmed by measurements of the P_{700} photochemical activity. The loss of activity was the result of two processes: loss of PSI core proteins and changes in the organization of PSI complexes. Blue native-polyacrylamide gel electrophoresis analysis revealed a Mn limitation-dependent dissociation of PSI trimers into monomers. The sensitive range for changes in the organization of the photosynthetic apparatus overlaps with the range of Mn concentrations measured in natural environments. We suggest that the ability to manipulate PSI content and organization allows cyanobacteria to balance electron transport rates between the photosystems. At naturally occurring Mn concentrations, such a mechanism will provide important protection against light-induced damage.

Manganese (Mn) is one of the most abundant transition metals in the Earth's crust and is vital for all known organisms (Frausto da Silva and Williams, 2001; Hänsch and Mendel, 2009). Mn ions are important cofactors for a number of enzymes, many of which catalyze reactions involving different oxygen species, such as Mn superoxide dismutase (Asada et al., 1975; Hänsch and Mendel, 2009), Mn peroxidase (Kenkebashvili et al., 2009), and catalase (Kono and Fridovich, 1983). In photosynthetic organisms, Mn plays a critical role in forming a cluster of four atoms on the donor side of PSII, which participates in catalyzing the water-splitting reaction. The cluster forms coordinative bonds with calcium and chloride ions and with residues of the D1 and CP43 proteins (Barber, 2008). Additional extrinsic proteins protect the Mn cluster from the aqueous environment of the lumen and form channels for water and oxygen diffusion. In cyanobacteria, these include the PsbO, PsbV (cytochrome c_{550}), and PsbU proteins and potentially two more, PsbQ and PsbP (Thornton et al., 2004; Roose et al., 2007).

Details on the cellular components involved in Mn transport through the outer and inner membranes of the gram-negative cyanobacteria are limited. The cyanobacterium *Synechocystis* sp. strain PCC 6803 (henceforth *Synechocystis* 6803) can accumulate up to 10^8 Mn^{2+} atoms per cell in its envelope layer. This pool is used as a reservoir for intracellular Mn, which is kept constant at approximately 10^6 atoms per cell. It was estimated that a large fraction of the intracellular pool is associated with PSII. Photosynthesis plays an important role in driving the envelope layer Mn accumulation process, as it does not occur in darkness and is blocked by PSII inhibitors (Keren et al., 2002). A periplasmic Mn-binding protein, MncA, was recently discovered by Tottey et al. (2008), but it remains to be determined whether its function is related to envelope layer Mn accumulation. The Mn transport route through the plasma membrane under Mn-sufficient conditions is not known. Under Mn-limiting conditions, Mn transport is carried out by the MntABC transporter (Bartsevich and Pakrasi, 1995, 1996).

In the late 1960s, Cheniae and Martin (1967, 1969) demonstrated that Mn limitation in cyanobacteria resulted in a reduction in oxygen evolution capacity. Addition of Mn restored oxygen evolution rates in a light-dependent process termed photoactivation. This process involves the sequential oxidation and coordinative bonding of the four Mn atoms, calcium and chloride ions to the C terminus of the mature D1 protein, and the CP43 subunit of PSII (for review, see Burnap, 2004; Dasgupta et al., 2008).

Despite the crucial role of Mn in the oxygen evolution process, it is not considered a limiting factor in aqueous environments. Mn concentrations in oceans and lakes are in the nanomolar range (Chester and Stoner, 1974; Sunda and Huntsman, 1988; Sterner et al., 2004; Morel, 2008), most of it in the form of bioavailable hydrated Mn^{2+}. In different recipes of the standard cyanobacterial growth medium BG11 (Allen, 1968), Mn concentrations range between 4 and 10 μM, approximately 3 orders of magnitude higher.

In this work, we examined the response of the photosynthetic apparatus in *Synechocystis* 6803 to Mn concentrations in the physiologically relevant range. Our results indicate that naturally occurring Mn concentrations can limit photosynthesis. The effects exerted by this limitation were not restricted to PSII. In parallel with the influence on PSII, Mn limitation induced changes in PSI content, oligomerization state, and function.

RESULTS

Effects on Biomass Accumulation, Primary Productivity, and Pigment Composition

To examine the response of *Synechocystis* 6803 to Mn limitation, we grew cultures in modified BG11 medium (YBG11; Shcolnick et al., 2007). YBG11-0, containing no added Mn, was supplemented with $MnCl_2$ to concentrations ranging from 0 to 10 μM. No significant effects on growth rate or on the physiology of the cells could be observed in the 10 to 1 μM range (data not shown), and our analysis focused on the 1 to 0 μM concentration range. Cells grown on Mn concentrations lower than 100 nM contained 60% to 70% lower intracellular Mn quotas (atoms per cell) as compared with cells grown on concentrations above this threshold (Supplemental Table S1).

Biomass accumulation and oxygen evolution decreased considerably below the 100 nM Mn threshold (Fig. 1). A similar Mn-dependent decrease in primary productivity was reported by Cheniae and Martin (1967) in studies of the cyanobacterium *Anacystis nidulans* R2. Nevertheless, the cellular chlorophyll quota remained relatively constant and changed by no more than 10% over the 1 to 0 μM range (Fig. 1B).

Effects on PSII Function

The effect on oxygen evolution rates suggested a change in the function of PSII. To gain further insight
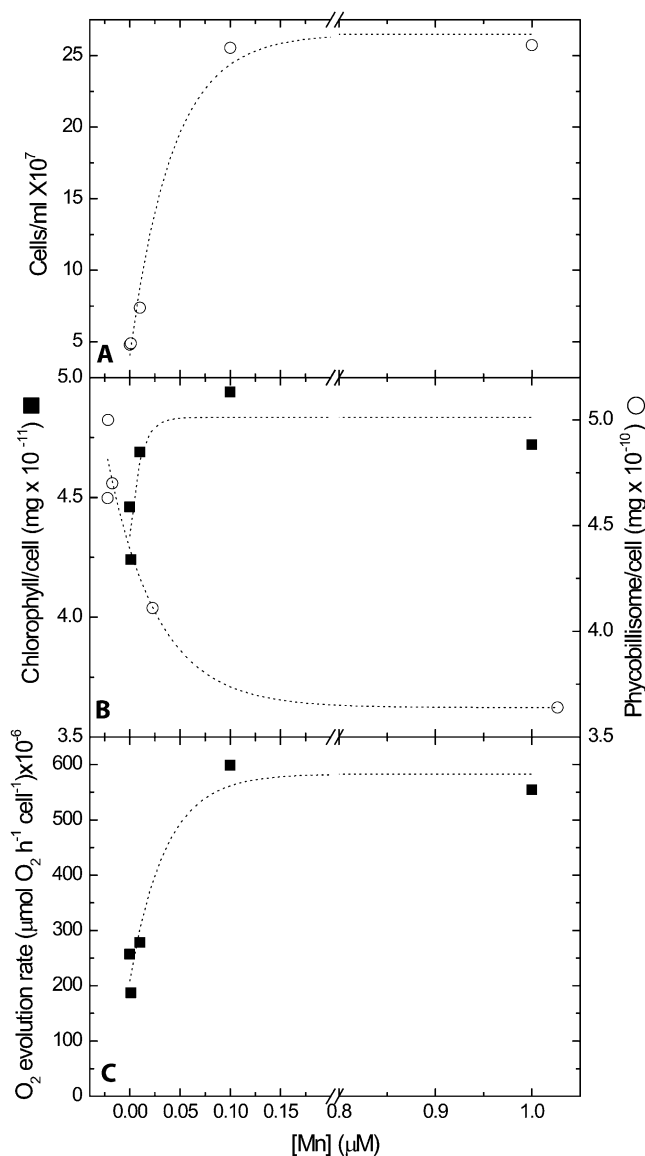
Figure 1. Effects of Mn availability on biomass accumulation, pigment content, and oxygen evolution rates. Starter cultures grown on 1 μM Mn medium were washed twice and transferred to YBG11-0 supplemented with 1 to 0 μM Mn, as indicated. The cultures were analyzed after 12 d of growth. A, Biomass accumulation (cells mL^{-1}). Cultures were inoculated at 10^6 cells mL^{-1}. B, Chlorophyll and phycobilisome content calculated on a per cell basis. In the data presented here, chlorophyll per cell values of cells grown on 0 μM were 90% of those grown on 1 μM Mn. In four independent repeats, measured after 18 to 21 d, this difference averaged 100% ± 14%. C, Maximal oxygen evolution rates, calculated on a per cell basis. Measurements were carried out in the presence of DMBQ and ferricyanide at a saturating light intensity. Experiments were repeated three times with comparable results. The reduction in biomass was strongly correlated with the reduction in intracellular Mn quotas (Supplemental Table S1; correlation coefficient of 0.99). The rate of PSII-dependent oxygen evolution (in C) was also strongly correlated to the intracellular Mn quota (correlation coefficient of 0.98).

into the response of PSII to Mn limitation, we measured the reoxidation rate of the primary electron-accepting plastoquinone of PSII (Q_A) following a saturating flash (Fig. 2). The maximal photosynthetic yield of PSII (F_v/F_m) decreased with decreasing Mn concentrations (Fig. 2A, inset). A similar reduction in F_v/F_m values was observed in hydroxyl-amine-treated cells, a procedure that removes the Mn cluster (Hwang et al., 2008). The rate of fluorescence relaxation, following the saturating flash, is indicative of the rate of Q_A reoxidation. In the absence of 3-(3,4-dichlorophenyl)-1,1-dimethylurea (DCMU), the rate of Q_A reoxidation is governed by the rate of forward electron transfer from the Q_A to the Q_B quinone-binding site. This rate was not affected by the reduction in intracellular Mn (Fig. 2A). In the presence of DCMU, which binds to the Q_B site, the rate of Q_A reoxidation is governed by the rate of recombination of the electron residing in the Q_A site with the hole residing on the donor side of PSII. The rate of this back reaction was much slower in cells grown on Mn concentrations above the 100 nM threshold than in cells grown on Mn concentrations below the threshold (Fig. 2B). Q_A reoxidation in the presence of DCMU can be described in terms of double exponential decay kinetics. In Figure 2C, we quantified changes in the rate of recombination as the ratio of the deconvoluted slow/fast decay phases. In the absence of an active donor, charge separation is not expected to progress beyond Y_Z^+/Q_A^-, an electron/hole pair that will recombine much faster than S_2/Q_A^-. Taken together, the faster rates of charge recombination (Fig. 2) and the reduction in oxygen evolution rates (Fig. 1C) indicated an effect on the energetic properties of the donor side of PSII in Mn-limited cultures. On immunoblots using an anti-D1 antibody, we could detect a small decrease in the abundance of this reaction center protein in Mn-limited cultures (Fig. 2D). Nevertheless, accumulation of unprocessed pD1 was not observed. The C-terminal extension of D1 prevents the binding of Mn and extrinsic proteins to PSII (Roose and Pakrasi, 2004). The results presented here indicate that while binding requires processing, the processing itself is not dependent on the presence of Mn.
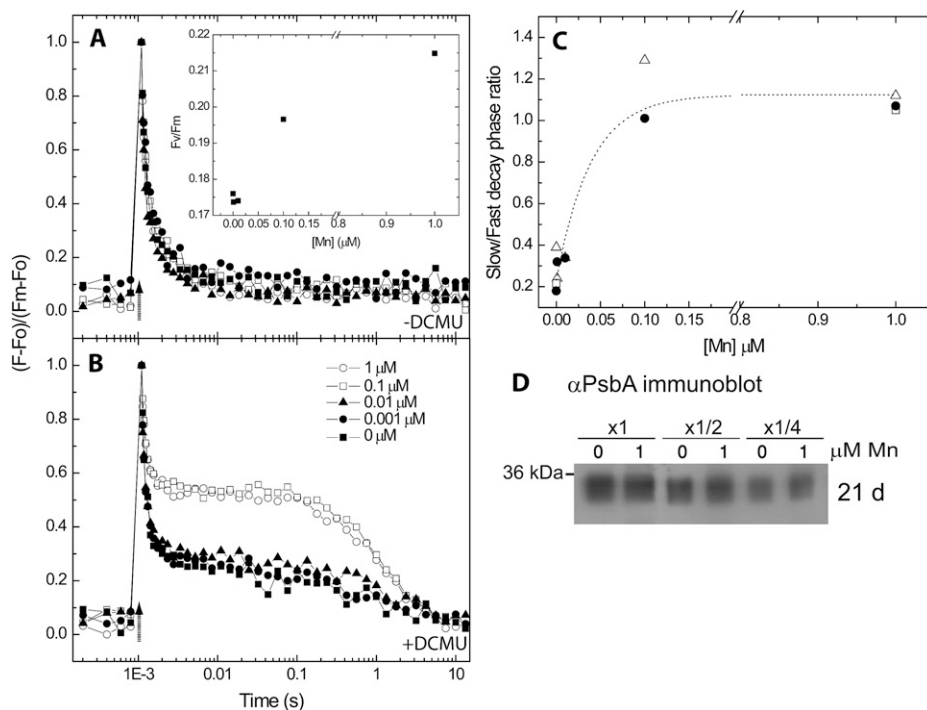
Figure 2. Effects of media Mn availability on the activity of PSII. A and B, *Synechocystis* 6803 cells, grown on a range of Mn concentrations as described in Figure 1, were analyzed for their rates of Q_A^- reoxidation following a single-turnover saturating flash (at the position marked by an arrow). Changes in fluorescence yield were monitored by a series of weak measuring flashes. The experiment was performed in the absence (A) or presence (B) of 10 μM DCMU. The data were normalized to the minimal and maximal fluorescence values. F_v/F_m values are presented in the inset in A. The decay of the signal following the flash in the presence of DCMU was fitted by a double exponential decay with a slow (0.9–1.5 s) and a fast (0.1–0.2 ms) phase. The r^2 values for the fits were greater than 0.95. C, The ratio of the slow/fast phase as a function of the Mn concentration. The ratio is calculated from data collected in three independent experiments. The data were fitted with an exponential trend line for clarity. D, Immunoblot analysis of PsbA (D1) levels. Proteins extracted from cells grown on YBG11 containing 1 or 0 μM Mn for 21 d were loaded on an equal chlorophyll basis. As a control, the samples were loaded at one-half and one-fourth of the original sample volume. The results were quantified using densitometry. D1 levels in 0 μM cultures were in the range of 88% ± 10% of the levels in the 1 μM cultures (n = 4).

Further support for the presence of PSII harboring a nonfunctional donor side was provided by 77 K chlorophyll fluorescence spectroscopy (Fig. 3A). Under Mn-limiting conditions, the fluorescence intensity of the peak at 682 nm increased significantly (Fig. 3, A and C). Fluorescence at this wavelength can arise from a number of sources, including the phycobilisome linker (Yamanaka et al., 1982), the IsiA protein (Burnap et al., 1993), and partially assembled PSII complexes (Seibert et al., 1988; Keren et al., 2005). Since the excitation wavelength was set at 430 ± 5 nm, the contribution of phycobilsomes can be excluded (Hwang et al., 2008). The contribution of IsiA to the 682-nm band was examined in the $\Delta isiA$ mutant (Fig. 3B). Under iron limitation, no change in fluorescence at 682 nm was observed in the mutant, as would be expected (Burnap et al., 1993). However, under Mn limitation, a distinct increase in fluorescence at this wavelength could be observed, indicating that the increase in the 682-nm band is not related to the IsiA protein. Therefore, the origin of the signal can only be the result of an accumulation of partially assembled PSII complexes. Similar 682-nm peaks were observed in partially assembled isolated PSII complexes (Seibert et al., 1988), purified plasma membranes (Keren et al., 2005), and mutants in the D1 processing protease CtpA in vivo (Shestakov et al., 1994; Keren et al., 2005). Surprisingly, changes in the spectra were not limited to the PSII region. With decreasing Mn concentrations, we observed a decrease in the relative intensity of fluorescence at 720 nm (Fig. 3, A and C). At this wavelength, the signal is dominated by PSI fluorescence (Papageorgiou, 2004). These results prompted us to take a closer look at the function of PSI.

Effects on PSI Function

The capacity for PSI photochemical activity was measured in vivo by P_{700} absorbance changes in the presence of DCMU (Fig. 4A). On a per-cell basis, the maximal P_{700} signal decreased with decreasing Mn concentrations (Fig. 4B). As in the case of oxygen evolution and Q_A reoxidation, a significant drop in activity was observed below the 100 nm threshold (Fig. 4, B and C). The loss of P_{700} photochemical activity developed gradually over a time course of 3 weeks following the transfer of cultures from 1 to 0 μM medium (Fig. 4C, inset).

The loss of activity was accompanied by a degradation of PSI proteins, as evidenced by the loss of the core PsaA protein and the accumulation of a 52-kD degradation fragment (Fig. 4D). This fragment is similar in size to the PsaA fragment that accumulates as a result of low-temperature PSI photodamage in cucumber (*Cucumis sativus*; Kudoh and Sonoike, 2002).

Organization of the Photosynthetic Apparatus

In addition to changes in the content of PSI, we detected differences in the oligomerization state of the photosynthetic complexes using blue native (BN)-
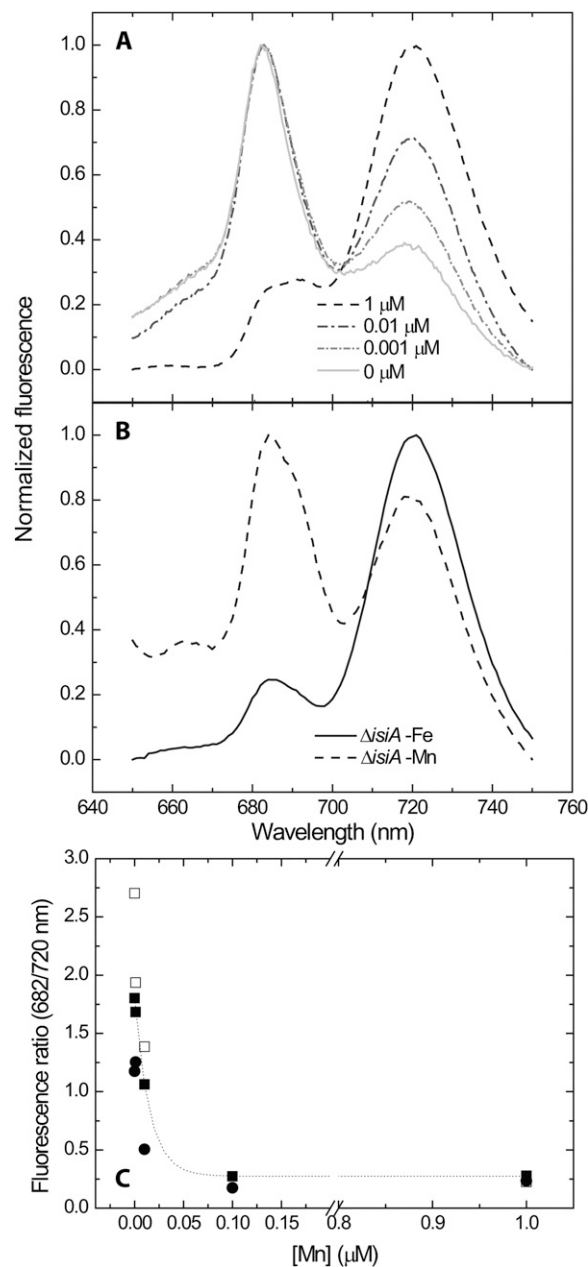
Figure 3. Low-temperature chlorophyll fluorescence spectroscopy. *Synechocystis* 6803 cells, prepared as in Figure 1, were collected and frozen in liquid nitrogen for analysis. Excitation wavelength was set at 430 ± 5 nm. A, Fluorescence spectra of wild-type cells grown on different Mn concentrations. B, Spectrum of the $\Delta isiA$ cells grown on iron (Fe)- or Mn-depleted YBG11 medium for 7 d. Longer incubation of $\Delta isiA$ cultures in YBG11-iron resulted in the collapse of the culture. C, Ratio of the peak intensities at 682 and 720 nm, calculated from data collected in three independent experiments performed on wild-type cultures.

PAGE (Fig. 5). In cells grown on 1 μM Mn, we could observe PSI trimers, monomers, and dimers. In addition, we detected PSII monomers. At the low *n*-dodecylmaltoside-chlorophyll ratios used here, PSII dimers were not expected (Takahashi et al., 2009; Watanabe et al., 2009).
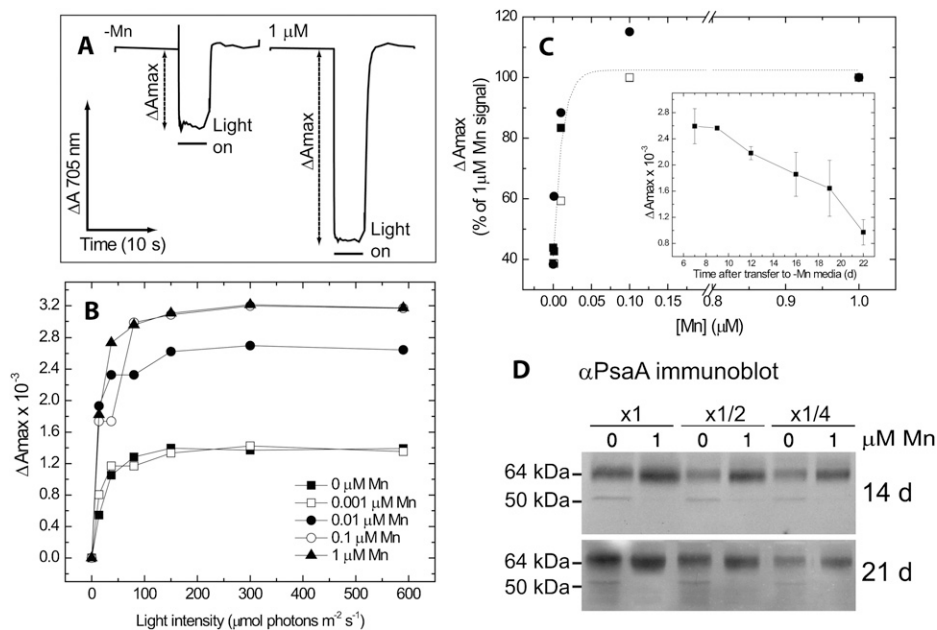
Figure 4. PSI photochemical activity and protein levels. P_{700} photochemical activity was measured in vivo in cultures grown on a range of Mn concentrations. Data were collected on an equal cell concentration basis. DCMU at 10 μM was added to block PSII activity. P_{700} oxidation was measured as the absorbance changes at 705 nm over a range of actinic light intensities. A, Samples of raw data from cultures grown on 0 or 1 μM Mn measured at 590 μmol photons m^{-2} s^{-1}. The data presented in B and C are absolute values of the maximal extent of the signal recorded (ΔAmax) as indicated in A. B, ΔAmax plotted as a function of the actinic light intensity for cultures grown on a range of Mn concentrations for 21 d. C, ΔAmax (measured at 590 μmol photons m^{-2} s^{-1}) as a function of medium Mn concentrations. The results are presented as percentages of the value for 1 μM. Data were collected from three independent experiments. The inset shows a time course of changes in ΔAmax following transfer from 1 to 0 μM Mn medium. The data were collected from two repeats. After 22 d, ΔAmax of the deficient cultures decreased to 42% of the value recorded in control Mn-sufficient cultures. D, Immunoblot analysis of PsaA levels. Proteins extracted from cells grown on YBG11 containing 1 or 0 μM Mn were loaded on an equal chlorophyll basis. As a control, the samples were loaded at one-half and one-fourth of the original sample volume. After 14 d of incubation, the PsaA content of 0 μM samples was 65% to 75% that of 1 μM samples ($n = 2$). Extending the incubation to 21 d did not result in any further change in the PsaA content of 0 μM samples as compared with 1 μM samples ($n = 2$).

Decreasing Mn bioavailability resulted in a small upshift in the mobility of the band containing PSI and PSII monomers (Fig. 5). Mass spectrometric analysis verified the presence of both PSI and PSII proteins in the shifted band (Supplemental Table S2). The higher oligomeric states of PSI (dimers, trimers, and super-complexes) changed significantly in response to Mn bioavailability. After 3 weeks of growth in Mn-limited medium, the level of these PSI complexes decreased to negligible amounts, leaving only PSI monomers (Fig. 5A). Similar results were obtained with membranes solubilized with the mild detergent digitonin (Supplemental Fig. S1). As with the P_{700} signal, the effect of Mn limitation developed gradually over time in cultures transferred from 1 to 0 μM Mn medium. Over a 21-d period, most of the PSI trimers were converted into monomers (Fig. 5B). Addition of Mn after 21 d resulted in the reappearance of the trimers (Fig. 5B).

The time scale for recovery from Mn limitation was assessed using 77 K spectroscopy, oxygen evolution, and P_{700} absorption (Fig. 6). After the addition of Mn to a limited culture, a gradual decrease in the relative intensity of the peak at 682 nm and an increase in the

relative intensity of the 720-nm peak were observed over a time scale of hours (Fig. 6). In parallel, the extent of the P_{700} signal and the rates of whole chain oxygen evolution increased (Fig. 6). In the Mn-limited state, oxygen evolution rates are restricted by PSII activity. Following recovery, oxygen evolution rates are limited downstream of PSII, as evident by the increase of the rate measured in the presence of artificial acceptors.

DISCUSSION

The data presented in this paper demonstrate a concerted response of the photosynthetic apparatus to limitation in intracellular Mn quotas. With declining Mn concentrations, PSII oxygen evolution rates dropped (Fig. 1C), Q_A reoxidation rates in the presence of DCMU increased (Fig. 2B), and the 682-nm band in the 77 K chlorophyll fluorescence spectra was enhanced (Fig. 3). These results indicated an accumulation of partially assembled PSII complexes lacking a functional donor side. Similar results were reported for Mn-limited Arabidopsis plants, where lower F_v/F_m
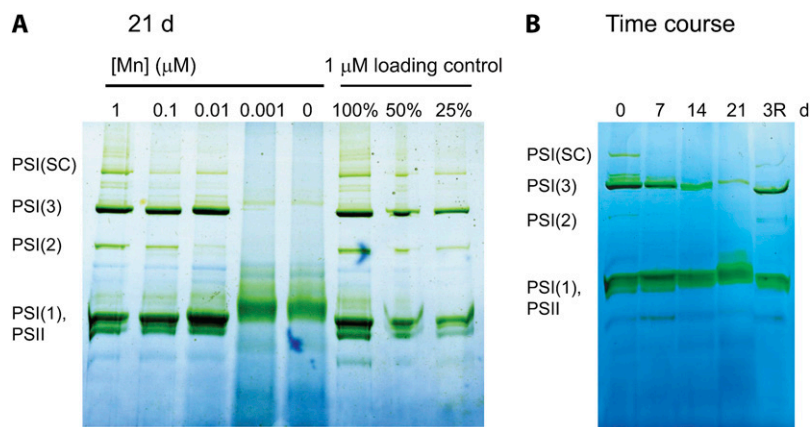
Figure 5. BN-PAGE analysis of the oligomeric state of membrane protein complexes. A, Reorganization of thylakoid membrane complexes in response to changes in Mn bioavailability. Cultures were grown on medium containing 0 to 1 μM Mn for 21 d. Membrane protein complexes were solubilized using a ratio of 0.03 g of *n*-dodecylmaltoside to 1 g of chlorophyll. Each sample contained 5 μg of chlorophyll. The identification of proteins in the different membrane complexes [PSII, PSI(1), PSI(2), PSI(3), and PSI(SC) supercomplexes] was performed by peptide mass spectrometry. Full details of the tryptic peptides identified in each band can be found in Supplemental Table S2. As a loading control, 100%, 50%, and 25% of the 1 μM samples were run alongside of the 0 μM sample. Based on these controls, we could estimate that the PSI trimer content in the 0 μM sample is considerably smaller than 25% of the 1 μM trimer content. B, Time course of the reorganization of thylakoid membrane complexes during the transition in and out of Mn limitation. Mn-sufficient cells were transferred to YBG11-0. Samples were taken and analyzed by BN-PAGE over a 0- to 21-d period, as indicated. Immediately after the last sample was collected on day 21, $MnCl_2$ was added to the remaining cells to a final concentration of 1 μM. The final sample was harvested 3 d after Mn repletion (3R). [See online article for color version of this figure.]

values and a damped PSII thermoluminescence oscillation profile were observed (Lanquar et al., 2010).

Considering that the overall content of D1 exhibited only a small decrease in Mn-deprived cells, we suggest that PSII complexes, containing a processed D1, are synthesized and await completion of the assembly process until Mn is available. Donor-side deficient PSII does not bind phycobilisomes efficiently (Hwang et al., 2008). Therefore, while the phycobilisome content in Mn-limited cells increased (Fig. 1B), partially assembled PSII will have some protection against photoinactivation due to a smaller absorption cross-section as compared with fully assembled PSII.

Although Mn is not a PSI cofactor, we observed a decrease in the fluorescence band at 720 nm associated mostly with PSI and in P_{700} photochemical activity (Figs. 3 and 4, respectively).

Reduction in PSI activity can be the result of two processes, loss of core proteins (Fig. 4D) and changes in the oligomerization state of PSI complexes. Under limiting Mn concentrations, PSI trimers disappeared while monomers persisted (Fig. 5; Supplemental Fig. S1; Supplemental Table S2). The lower activity of the monomers can be attributed to two factors: loss of long-wavelength chlorophylls in the monomers (El-Mohsnawy et al., 2010) and excitation spillover to PSII. As compared with trimers, PSI monomers have a much higher probability for interactions with PSII (in trimers, two out of the three membrane-embedded surfaces of the monomer are locked in PSI-PSI interactions). Close interactions promote direct energy transfer between PSII and PSI, a process often referred to as spillover (McConnell et al., 2002). Transfer of energy between the photosystems may provide additional defense against photooxidative damage to PSII under limited Mn bioavailability. PSI monomers can quench PSII excitation and reduce the risk of damage from reactive oxygen species.

Trimers are considered the dominant form in cyanobacteria, and the transition toward fully functional monomeric PSI most probably took place only after endosymbiosis (Nelson, 2009). However, there are reports of an active interplay between monomers and trimers in cyanobacteria. These include studies conducted by the Rogner group (Kruip et al., 1994; El-Mohsnawy et al., 2010), who were able to manipulate the PSI oligomerization state in membranes by changing the ionic strength, which led to the suggestion that changes in the oligomeric organization are related to state transition. Ivanov et al. (2006) reported an accumulation of PSI monomers at the early stages of iron limitation. As in the work of Kruip and coworkers (1994), the monomerization of trimeric PSI was suggested to be associated with a reduction in the coupling with phycobilisomes, yielding a smaller PSI absorption cross-section and lower PSI activity.

The Mn bioavailability-dependent reduction in the content of both photosystems was not accompanied by a decrease in the cellular chlorophyll content (Fig. 1B). Chlorophyll is considerably more stable than photosystem proteins in cyanobacteria. Its half-life in wild-type cells is longer than 200 h. The stability is associated
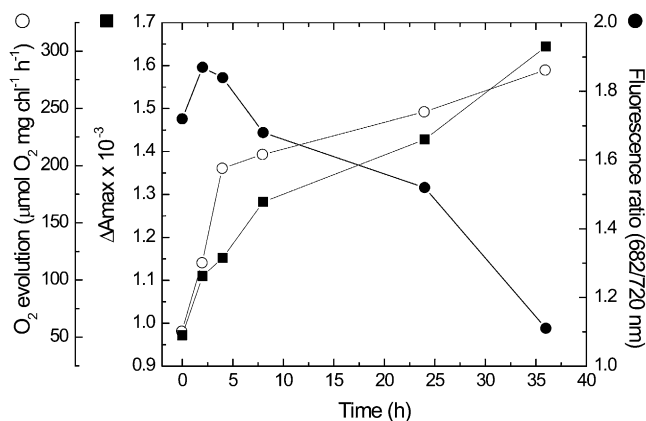
Figure 6. Time course of recovery from Mn limitation. *Synechocystis* 6803 cells were grown on YBG11-0 for 14 d. At time zero, MnCl$_2$ was added to a final concentration of 1 μM. Oxygen evolution rates (white circles), P$_{700}$ ΔAmax (black squares), and the 682/720-nm 77 K chlorophyll fluorescence intensity ratio (black circles) were monitored throughout the recovery phase. Oxygen evolution was measured in the absence of artificial acceptors. The addition of DMBQ and ferricyanide to limited cells improved the oxygen evolution rate by 5%. At 24 h into the recovery process, the addition of acceptors improved the rate by 65%.

with the function of small Cab-like proteins that bind free chlorophyll and protect it from degradation (Vavilin et al., 2007). Chlorophyll bound to small Cab-like proteins can be recycled into newly formed photosystems in the process of recovery from Mn limitation. Recovery occurs on the time scale of hours to days (Figs. 5B and 6). The rate of recovery can be compared with the rate of Mn transport, which was calculated to be in the 10^5 atoms cell^{-1} h^{-1} range (Keren et al., 2002). With 1.5 $\times$ 10^6 Mn atoms per cell in replete cultures and 4.5 $\times$ 10^5 atoms per cell in limited cultures (Supplemental Table S1), it is reasonable to assume that the limiting factor in the recovery process is the rate of Mn transport.

CONCLUSION

For both PSII and PSI, Mn limitation did not result in the induction of extensive protein degradation processes similar to those observed under prolonged iron limitation (Sherman and Sherman, 1983; Yeremenko et al., 2004) or nitrogen limitation (Schwarz and Grossman, 1998). Unlike iron or nitrogen, redirecting Mn from photosynthesis toward other cellular processes will serve little purpose. The genome of *Synechocystis* 6803 does not code for a Mn superoxide dismutase (Kaneko et al., 1996; http://genome.kazusa.or.jp/cyanobase). In other cyanobacterial species, Mn requirements for superoxide dismutase can be offset by iron (Morel, 2008).

By and large, nitrogen, phosphate, and iron are considered the major limiting factors for primary productivity in water bodies. This is not the case with Mn (Morel, 2008). Nevertheless, the nanomolar

Mn concentration range of both freshwater and saltwater bodies (Chester and Stoner, 1974; Sunda and Huntsman, 1988; Sterner et al., 2004; Morel, 2008) is within the sensitive range for changes in photosynthetic activity observed here. The 4.5 to 22 μM Mn concentration used in standard cyanobacterial growth media (e.g. BG11, A+, and ASP2), under which PSII is fully active and PSI is mostly trimeric, does not accurately represent the situation in nature. Under natural conditions, the activity, oligomeric state, and membrane distribution of the photosystems will fluctuate in response to small changes in Mn concentrations. While limitation of growth rate may result from processes downstream of the electron transfer chain altogether (Raven, 1990), the reduced activity and changes in spatial organization should be considered in studies of the function of the photosynthetic apparatus. Furthermore, this partially active state of the photosynthetic apparatus has implications for ecological studies of primary productivity, especially when nutrient colimitation scenarios are taken into account.

MATERIALS AND METHODS

Cyanobacterial Strains and Culture Conditions

Wild-type *Synechocystis* 6803 cultures were grown in 50 to 150 mL of YBG11 medium (Shcolnick et al., 2007) in 250- or 500-mL glass Erlenmeyer flasks, respectively. Cultures were maintained under constant shaking and illumination of 60 μmol photons m^{-2} s^{-1} at 30°C. In YBG11 medium with no added MnCl$_2$ (YBG11-0), Mn contamination levels were below the detection limit in our inductively coupled plasma mass spectrometer measurements, 0.1 μg L^{-1} or 1.8 nM. Starter cultures were grown on YBG11 containing 1 μM Mn for 3 d to reduce contaminations during subsequent growth in limiting medium. In order to remove excess Mn, cultures were washed twice in 20 mM MES, 10 mM EDTA, pH 5.0 buffer (Keren et al., 2002). The cells were resuspended in YBG11-0. Equal aliquots were transferred to flasks containing YBG11-0 supplemented with MnCl$_2$ to the desired concentration. Glassware was incubated overnight in 3.7% HCl and then washed with double distilled water. The ΔisiA mutant (Singh et al., 2005) was grown on medium containing kanamycin but was assayed in the same medium as wild-type cultures. Cell densities were measured as optical density at 730 nm using a Cary3000 spectrophotometer (Varian) as described previously (Shcolnick et al., 2007). Pigment content was calculated from in vivo absorption measurements as described by Arnon et al. (1974). The effects of Mn limitation developed gradually as a function of media Mn concentrations and time of incubation. These parameters are reported in all of the figure legends.

Oxygen Evolution Measurements

Synechocystis 6803 cells grown on the various Mn concentrations were brought to the same cell density. Oxygen evolution rates were measured using a Clark-type electrode (Pasco). All measurements were carried out under saturating light at 30°C. Where indicated, 5 μM 2,6-dimethyl-*p*-benzoquinone (DMBQ) and 5 mM ferricyanide were added.

Spectroscopic Analysis

Q$_A$ reoxidation was measured using a Fluorowin2000 fluorometer (Photon Systems Instruments). DCMU was added to a final concentration of 10 μM. Measurements of this type suffer from a fast-decaying signal arising from the flash itself. To avoid this artifact, the first data point following the flash was measured after a delay of 110 μs.

The decay phase of the curves was deconvoluted using a double exponential decay equation:

$$y = y_0 + A_1 \times 10^{(-t_1/t)} + A_2 \times 10^{(-t_2/t)}$$

where t is time (s), y is fluorescence intensity, y_0 is F_o fluorescence intensity, A_1 and A_2 are preexponential factors representing the extent of the decay phase, and t_1 and t_2 are decay time constants.

Chlorophyll fluorescence at 77 K was measured using a Flouromax3 spectrofluorometer (Jobin Ivon) with the excitation wavelength set at 430 ± 5 nm and a 5-nm emission window. The values presented were internally normalized to the maximum and minimum values of each curve. P_{700} photoreduction was measured in vivo in cultures adjusted to an optical density at 730 nm of 0.5. DCMU was added to a final concentration of 10 μM. Measurements were performed using a Joliot-type spectrophotometer (JTS-10; Bio-Logic) using an optical path of 10 mm. Excitation was provided by green light-emitting diodes (Rappaport et al., 2007), and the response of PSI was measured at 705 nm as described by Joliot and Joliot (2005).

Protein Analysis and Mass Spectrometric Determination

For protein separation using BN-PAGE and SDS-PAGE techniques, *Synechocystis* 6803 cells were broken by rigorous bead beating, and the resulting thylakoid membranes were collected by centrifugation as described by Gombos et al. (1994). Thylakoid membranes were resuspended in a buffer containing 330 mM mannitol, 30 mM HEPES, 2 mM EDTA, and 3 mM MgCl$_2$, pH 7.8. Linear 4.5% to 12% BN-PAGE was performed as described by Heinemeyer et al. (2004) using the mild detergent *n*-dodecylmaltoside in a ratio of 0.03:1 (w/w) *n*-dodecylmaltoside:chlorophyll. Identification of the components of bands cut out of BN-PAGE gels was performed by mass spectrometric measurements (Supplemental Table S2). SDS-PAGE and immunodetection were performed as described by Laemmli (1970) using antibodies produced by Agrisera.

The elemental composition of the cells was determined as described by Shcolnick et al. (2007). Extracellular iron was removed by two consecutive 15-min washes in 20 mM MES, 10 mM EDTA, pH 5.0. The cells were digested at 100°C with distilled HNO$_3$, evaporated to dryness, and reconstituted in double distilled water. Metal quotas were also determined using a SCIEX-CDR II inductively coupled plasma mass spectrometer (Perkin-Elmer).

Supplemental Data

The following materials are available in the online version of this article.

Supplemental Figure S1. BN-PAGE analysis of the oligomerization state of membrane protein complexes using the mild detergent digitonin.

Supplemental Table S1. Intracellular metal quotas of cells grown on a range of Mn media concentrations.

Supplemental Table S2. Mass spectrometric identification of proteins in green BN-PAGE bands.

LITERATURE CITED

Allen MM (1968) Simple conditions for growth of unicellular blue-green algae on plates. J Phycol **4:** 1–4

Arnon DI, McSwain BD, Tsujimoto HY, Wada K (1974) Photochemical activity and components of membrane preparations from blue-green algae. I. Coexistence of two photosystems in relation to chlorophyll *a* and removal of phycocyanin. Biochim Biophys Acta **357:** 231–245

Asada K, Yoshikawa K, Takahashi MA, Maeda Y, Enmanji K (1975) Superoxide dismutases from a blue-green alga, *Plectonema boryanum*. J Biol Chem **250:** 2801–2807

Barber J (2008) Crystal structure of the oxygen-evolving complex of photosystem II. Inorg Chem **47:** 1700–1710

Bartsevich VV, Pakrasi HB (1995) Molecular identification of an ABC transporter complex for manganese: analysis of a cyanobacterial mutant strain impaired in the photosynthetic oxygen evolution process. EMBO J **14:** 1845–1853

Bartsevich VV, Pakrasi HB (1996) Manganese transport in the cyanobacterium *Synechocystis* sp. PCC 6803. J Biol Chem **271:** 26057–26061

Burnap RL (2004) D1 protein processing and Mn cluster assembly in light of the emerging photosystem II structure. Phys Chem Chem Phys **6:** 4803–4809

Burnap RL, Troyan T, Sherman LA (1993) The highly abundant chlorophyll-protein complex of iron-deficient *Synechococcus* sp. PCC7942 (CP43′) is encoded by the isiA gene. Plant Physiol **103:** 893–902

Cheniae GM, Martin IF (1967) Photoreactivation of manganese catalyst in photosynthetic oxygen evolution. Biochem Biophys Res Commun **28:** 89–95

Cheniae GM, Martin IF (1969) Photoreaction of manganese catalyst in photosynthetic oxygen evolution. Plant Physiol **44:** 351–360

Chester R, Stoner JH (1974) The distribution of zinc, nickel, manganese, cadmium, copper and iron in some surface waters from the world ocean. Mar Chem **2:** 17–32

Dasgupta J, Ananyev GM, Dismukes GC (2008) Photoassembly of the water oxidizing complex in photosystem II. Coord Chem Rev **252:** 347–360

El-Mohsnawy E, Kopczak MJ, Schlodder E, Nowaczyk M, Meyer HE, Warscheid B, Karapetyan NV, Rögner M (2010) Structure and function of intact photosystem 1 monomers from the cyanobacterium Thermosynechococcus elongatus. Biochemistry **49:** 4740–4751

Frausto da Silva JJR, Williams RJP (2001) The Biological Chemistry of the Elements. Oxford University Press, Oxford

Gombos Z, Wada H, Murata N (1994) The recovery of photosynthesis from low-temperature photoinhibition is accelerated by the unsaturation of membrane lipids: a mechanism of chilling tolerance. Proc Natl Acad Sci USA **91:** 8787–8791

Hänsch R, Mendel RR (2009) Physiological functions of mineral micronutrients (Cu, Zn, Mn, Fe, Ni, Mo, B, Cl). Curr Opin Plant Biol **12:** 259–266

Heinemeyer J, Eubel H, Wehmhöner D, Jänsch L, Braun HP (2004) Proteomic approach to characterize the supramolecular organization of photosystems in higher plants. Phytochemistry **65:** 1683–1692

Hwang HJ, Nagarajan A, McLain A, Burnap RL (2008) Assembly and disassembly of the photosystem II manganese cluster reversibly alters the coupling of the reaction center with the light-harvesting phycobilisome. Biochemistry **47:** 9747–9755

Ivanov AG, Krol M, Sveshnikov D, Selstam E, Sandström S, Koochek M, Park YI, Vasil'ev S, Bruce D, Oquist G, et al (2006) Iron deficiency in cyanobacteria causes monomerization of photosystem I trimers and reduces the capacity for state transitions and the effective absorption cross section of photosystem I in vivo. Plant Physiol **141:** 1436–1445

Joliot P, Joliot A (2005) Quantification of cyclic and linear flows in plants. Proc Natl Acad Sci USA **102:** 4913–4918

Kaneko T, Sato S, Kotani H, Tanaka A, Asamizu E, Nakamura Y, Miyajima N, Hirosawa M, Sugiura M, Sasamoto S, et al (1996) Sequence analysis of the genome of the unicellular cyanobacterium *Synechocystis* sp. strain PCC6803. II. Sequence determination of the entire genome and assignment of potential protein-coding regions (supplement). DNA Res **3:** 185–209

Kenkebashvili NV, Elisashvili V, Hadar Y (2009) Effect of nutrient medium composition on laccase and manganese peroxidase activity in medicinal mushrooms. Int J Med Mushrooms **11:** 191–198

Keren N, Kidd MJ, Penner-Hahn JE, Pakrasi HB (2002) A light-dependent mechanism for massive accumulation of manganese in the photosynthetic bacterium *Synechocystis* sp. PCC 6803. Biochemistry **41:** 15085–15092

Keren N, Liberton M, Pakrasi HB (2005) Photochemical competence of assembled photosystem II core complex in cyanobacterial plasma membrane. J Biol Chem **280:** 6548–6553

Kono Y, Fridovich I (1983) Isolation and characterization of the pseudo-catalase of Lactobacillus plantarum. J Biol Chem **258:** 6015–6019

Kruip J, Bald D, Boekema E, Rogner M (1994) Evidence for the existence of trimeric and monomeric photosystem I complexes in thylakoid membranes from cyanobacteria. Photosynth Res **40:** 279–286

Kudoh H, Sonoike K (2002) Irreversible damage to photosystem I by chilling in the light: cause of the degradation of chlorophyll after returning to normal growth temperature. Planta **215:** 541–548

Laemmli UK (1970) Cleavage of structural proteins during the assembly of the head of bacteriophage T4. Nature **227:** 680–685

Lanquar V, Ramos MS, Lelièvre F, Barbier-Brygoo H, Krieger-Liszkay A, Krämer U, Thomine S (2010) Export of vacuolar manganese by AtNRAMP3 and AtNRAMP4 is required for optimal photosynthesis and growth under manganese deficiency. Plant Physiol **152:** 1986–1999

McConnell MD, Koop R, Vasil'ev S, Bruce D (2002) Regulation of the distribution of chlorophyll and phycobilin-absorbed excitation energy in cyanobacteria: a structure-based model for the light state transition. Plant Physiol **130:** 1201–1212

Morel FMM (2008) The co-evolution of phytoplankton and trace element cycles in the oceans. Geobiology **6:** 318–324

Nelson N (2009) Plant photosystem I: the most efficient nano-photochemical machine. J Nanosci Nanotechnol **9:** 1709–1713

Papageorgiou GC (2004) Fluorescence of photosynthetic pigments *in vivo* and *in vitro*. *In* GC Papageorgiou, Govindjee, eds, Chlorophyll *a* Fluorescence, a Signature of Photosynthesis. Springer, Dordrecht, The Netherlands, pp 43–63

Rappaport F, Béal D, Joliot A, Joliot P (2007) On the advantages of using green light to study fluorescence yield changes in leaves. Biochim Biophys Acta **1767:** 56–65

Raven JA (1990) Predictions of Mn and Fe use efficiencies of phototrophic growth as a function of light availability for growth and of C assimilation pathway. New Phytol **116:** 1–18

Roose JL, Pakrasi HB (2004) Evidence that D1 processing is required for manganese binding and extrinsic protein assembly into photosystem II. J Biol Chem **279:** 45417–45422

Roose JL, Wegener KM, Pakrasi HB (2007) The extrinsic proteins of photosystem II. Photosynth Res **92:** 369–387

Schwarz R, Grossman AR (1998) A response regulator of cyanobacteria integrates diverse environmental signals and is critical for survival under extreme conditions. Proc Natl Acad Sci USA **95:** 11008–11013

Seibert M, Picorel R, Rubin AB, Connolly JS (1988) Spectral, photophysical, and stability properties of isolated photosystem II reaction center. Plant Physiol **87:** 303–306

Shcolnick S, Shaked Y, Keren N (2007) A role for mrgA, a DPS family protein, in the internal transport of Fe in the cyanobacterium *Synechocystis* sp. PCC 6803. Biochim Biophys Acta **1767:** 814–819

Sherman DM, Sherman LA (1983) Effect of iron deficiency and iron restoration on ultrastructure of *Anacystis nidulans*. J Bacteriol **156:** 393–401

Shestakov SV, Anbudurai PR, Stanbekova GE, Gadzhiev A, Lind LK, Pakrasi HB (1994) Molecular cloning and characterization of the ctpA gene encoding a carboxyl-terminal processing protease: analysis of a spontaneous photosystem II-deficient mutant strain of the cyanobacterium *Synechocystis* sp. PCC 6803. J Biol Chem **269:** 19354–19359

Singh AK, Li H, Bono L, Sherman LA (2005) Novel adaptive responses revealed by transcription profiling of a Synechocystis sp. PCC 6803 delta-isiA mutant in the presence and absence of hydrogen peroxide. Photosynth Res **84:** 65–70

Sterner RW, Smutka TM, McKay RML, Qin XM, Brown ET, Sherrell RM (2004) Phosphorus and trace metal limitation of algae and bacteria in Lake Superior. Limnol Oceanogr **49:** 495–507

Sunda WG, Huntsman SA (1988) Effect of sunlight on redox cycles of manganese in the southwestern Sargasso Sea. Deep-Sea Res **35:** 1297–1317

Takahashi T, Inoue-Kashino N, Ozawa S, Takahashi Y, Kashino Y, Satoh K (2009) Photosystem II complex *in vivo* is a monomer. J Biol Chem **284:** 15598–15606

Thornton LE, Ohkawa H, Roose JL, Kashino Y, Keren N, Pakrasi HB (2004) Homologs of plant PsbP and PsbQ proteins are necessary for regulation of photosystem II activity in the cyanobacterium *Synechocystis* 6803. Plant Cell **16:** 2164–2175

Tottey S, Waldron KJ, Firbank SJ, Reale B, Bessant C, Sato K, Cheek TR, Gray J, Banfield MJ, Dennison C, et al (2008) Protein-folding location can regulate manganese-binding versus copper- or zinc-binding. Nature **455:** 1138–1142

Vavilin D, Yao D, Vermaas W (2007) Small Cab-like proteins retard degradation of photosystem II-associated chlorophyll in Synechocystis sp. PCC 6803: kinetic analysis of pigment labeling with ^{15}N and ^{13}C. J Biol Chem **282:** 37660–37668

Watanabe M, Iwai M, Narikawa R, Ikeuchi M (2009) Is the photosystem II complex a monomer or a dimer? Plant Cell Physiol **50:** 1674–1680

Yamanaka G, Lundell DJ, Glazer AN (1982) Molecular architecture of a light-harvesting antenna: isolation and characterization of phycobilisome subassembly particles. J Biol Chem **257:** 4077–4086

Yeremenko N, Kouril R, Ihalainen JA, D'Haene S, van Oosterwijk N, Andrizhiyevskaya EG, Keegstra W, Dekker HL, Hagemann M, Boekema EJ, et al (2004) Supramolecular organization and dual function of the IsiA chlorophyll-binding protein in cyanobacteria. Biochemistry **43:** 10308–10313